Role of Tetanus Neurotoxin Insensitive Vesicle-associated Membrane Protein (TI-VAMP) in Vesicular Transport Mediating Neurite Outgrowth✪

Sonia Martinez-Arca,*‡ Philipp Alberts,*‡ Ahmed Zahraoui,‡ Daniel Louvard,‡ and Thierry Galli*‡

*Group of Membrane Traffic and Neuronal Plasticity, INSERM U536, and ‡Group of Morphogenesis and Cell Signaling, CNRS UMR144, Institut Curie, F-75005 Paris, France

Abstract. How vesicular transport participates in neurite outgrowth is still poorly understood. Neurite outgrowth is not sensitive to tetanus neurotoxin thus does not involve synaptobrevin-mediated vesicular transport to the plasma membrane of neurons. Tetanus neurotoxin-insensitive vesicle-associated membrane protein (TI-VAMP) is a vesicle-SNARE (soluble N-ethylmaleimide-sensitive fusion protein [NSF] attachment protein [SNAP] receptor), involved in transport to the apical plasma membrane in epithelial cells, a tetanus neurotoxin-resistant pathway. Here we show that TI-VAMP is essential for vesicular transport-mediating neurite outgrowth in staurosporine-differentiated PC12 cells. The NH_2-terminal domain, which precedes the SNARE motif of TI-VAMP, inhibits the association of TI-VAMP with synaptosome-associated protein of 25 kD (SNAP25). Expression of this domain inhibits neurite outgrowth as potently as Botulinum neurotoxin E, which cleaves SNAP25. In contrast, expression of the NH_2-terminal deletion mutant of TI-VAMP increases SNARE complex formation and strongly stimulates neurite outgrowth. These results provide the first functional evidence for the role of TI-VAMP in neurite outgrowth and point to its NH_2-terminal domain as a key regulator in this process.

Key words: membrane traffic • neurite outgrowth • SNAREs • TI-VAMP • SNAP25

Introduction

Elongation of axon and dendrites, so-called neurite outgrowth, is a crucial event in neuronal differentiation and maturation during development of the nervous system (Prochiantz, 1995). Neurite outgrowth relies primarily on the transport and addition of new components to the plasma membrane but little is known about the vesicle targeting and fusion machinery involved in this process (Futerman and Banker, 1996; Bradke and Dotti, 1997).

Membrane traffic can be envisioned as a succession of vesicle budding, maturation, vectorial transport, tethering, docking, and lipid bilayer fusion events. Vesicular transport to and fusion at the plasma membrane, i.e., exocytosis, is responsible for the release of soluble compounds, such as neurotransmitters in the extracellular medium, and for surface expression of plasma membrane proteins and lipids. Overwhelming evidence accumulated over the last years shows that soluble N-ethylmaleimide–sensitive fusion protein (NSF)[1] attachment protein (SNAP) receptors

(SNAREs) are key proteins of membrane traffic, most likely involved in lipid bilayer fusion (Weber et al., 1998; Nickel et al., 1999; Parlati et al., 1999; Bock and Scheller, 1999). Clostridial neurotoxins (NTs) carry a proteolytic activity, which selectively cleaves defined SNAREs. Hence they have been extensively used to demonstrate the involvement of NT-sensitive SNAREs in vesicular transport (for review, see Johannes and Galli, 1998).

Surprisingly, several exocytotic pathways are resistant to NTs, particularly to tetanus neurotoxin (TeNT), which cleaves several members of the synaptobrevin (also called vesicle-associated membrane protein, VAMP) family of SNAREs. TeNT resistance of the transport to the apical plasma membrane, in epithelial cells, was originally interpreted as the occurrence of SNARE-independent exocyto-

sis (Ikonen et al., 1995; Simons and Ikonen, 1997). A breakthrough resulted from the cloning of synaptobrevin-like gene 1 (D'Esposito et al., 1996) and the finding that its product is insensitive to TeNT and Botulinum NTs (BoNTs) B, D, F, and G (Galli et al., 1998). This protein, called TeNT-insensitive VAMP (TI-VAMP) or VAMP7, forms apical SNARE complexes and mediates fusion of vesicles with the apical plasma membrane (Galli et al., 1998; Lafont et al., 1999). It is also present in the degradation pathway of EGF in fibroblasts (Advani et al., 1999). TI-VAMP is a likely candidate for vesicle SNARE (v-SNARE) of NT-resistant exocytotic pathways. Interestingly, neurite outgrowth is resistant to TeNT, thus does not involve synaptobrevin and synaptic vesicles (SVs; Osen-Sand et al., 1996; AhnertHilger et al., 1996). Genetic evidences confirm this. First, in fly and nematode, elimination of the neuronal synaptobrevin leads to severe impairment of neurotransmitter release but has no effect on neurite outgrowth (Deitcher et al., 1998; Nonet et al., 1998). Second, neurite outgrowth is normal in a PC12 clone lacking synaptobrevins 1 and 2 (Leoni et al., 1999). In a previous study, we have shown that TI-VAMP–containing vesicular compartment excludes synaptobrevin 2 and other markers of well-characterized exocytic and endocytic compartments and it concentrates in the leading edge of axonal and dendritic processes in hippocampal neurons in primary culture (Coco et al., 1999). In this paper, we show that TI-VAMP fulfills the criteria to be the v-SNARE implicated in neurite outgrowth.

Materials and Methods

Antibodies and Clones

Rabbit serums (TG11 and TG16; Galli et al., 1998; Lafont et al., 1999) directed against TI-VAMP were purified by affinity chromatography in a column loaded with a GST fusion protein of the coiled-coil domain of TI-VAMP (see below). Mouse monoclonal antibodies directed against synaptobrevin 2 (clone 69.1, generous gift from R. Jahn, Max Planck Institute, Goettingen, FRG), SNAP25 (clone 20, Transduction Labs.), green fluorescent protein (GFP; clone 7.1 and 13.1, Boehringer), syntaxin 6 (clone 30, Transduction Labs), syntaxin 1 (HPC-1, generous gift from C. Barnstable, Yale University, New Haven, CT), glutathione-S-transferase (GST; generous gift from J.-L. Theillaud, Institut Curie, Paris, France), TeNT light chain (TeNT-LC; generous gift from H. Niemann, Hannover Medical School, Hannover, Germany), rabbit polyclonal antibodies against the ectoplasmic domain of synaptotagmin I (8907, generous gift from P. DeCamilli, Yale University, New Haven, CT), SNAP25 (MC9, generous gift from P. DeCamilli, Yale University, New Haven, CT), GFP (Boehringer), and histidine (Santa Cruz Biotechnology, Inc.) have been described previously. Affinity-purified Cy2 and Texas red–coupled goat anti–mouse and anti–rabbit immunoglobulins were purchased from Jackson Laboratory. Rhodamine-coupled phalloidin was from Sigma-Aldrich. Alkaline phosphatase-coupled sheep anti–mouse were from Promega. The cDNAs of human TI-VAMP and cellubrevin were previously described (Galli et al., 1998). The cDNAs of rat synaptobrevin 2 (R. Scheller, Stanford University, Stanford, CA), rat SNAP25A (R. Jahn, Max Planck Institute, Goettingen, Germany), TeNT-LC and BoNT-LC (H. Niemann, Hannover Medical School, Hannover, Germany) and ratiometric pHLuorin (G. Miesenbock, Sloan Kettering Memorial Hospital, New York, NY) were generous gifts.

Cell Culture

PC12 cells were cultured in RPMI supplemented with 10% horse serum (HS) and 5% FCS as described (Greene and Tischler, 1976). Cells were plated either on collagen-coated plastic dishes or on poly-L-lysine plus collagen-coated glass coverslips (Chilcote et al., 1995). HeLa cells were cultured in DME supplemented with 10% FCS.

DNA constructions: for production of NH_2-terminal GFP fusion proteins, the distinct cDNAs were cloned into the pEGFP-C3 vector (CLONTECH Laboratories, Inc.). The same empty vector was also used as a control in some of the neurite outgrowth assays. Full-length TI-VAMP (TIVAMP), NH_2-terminal domain-TIVAMP (Nter-TIVAMP, from M^1 to N^{120}), cytosolic domain-TIVAMP (Cyt-TIVAMP, from M^1 to K^{188}), ΔNH_2-terminal domain-TIVAMP (ΔNter-TIVAMP, from M^{102} to the end), and full-length synaptobrevin 2 (Sb2), were obtained by PCR using standard procedures and the following sets of oligonucleotides: 5′-ATG-GCGATTCTTTTTGCTGTTGTTGCC-3′ and 5′-CTATTTCTTCACA-CAGCTTGGCCATGT-3′ for TIVAMP; 5′-ATGGCGATTCTTTTTG-CTGTTGTTGCC-3′ and 5′-CTTATTCTCAGAGTGATGCTTCAG-CTG-3′ for Nter-TIVAMP; 5′-ATGGCGATTCTTTTTGCTGTTGT-TGCC-3′ and 5′-ATCCTACTTGAGGTTCTTCATACACATGGCTC for Cyt-TIVAMP; 5′-ATGAATAGCGAGTTCTCAAGTGTCTTA-3′ and 5′-CTATTTCTTCACACAGCTTGGCCATGT-3′ for ΔNter-TIVAMP; 5′-ATGTCGGCTACCGCTGCCACCGTCCCG-3′ and 5′-TTAAGAGCTGAAGTAAACTATGATGAT for Sb2. TIVAMP, Nter-TIVAMP, Cyt-TIVAMP, and Sb2 were cloned in pEGFP-C3 using the KpnI-XbaI sites, while ΔNter-TIVAMP was cloned in HindIII-XbaI sites.

For production of the COOH-terminal GFP (ratiometric pHLuorin in this case) fusion protein of TI-VAMP, TI-VAMP cDNA bearing a BamHI site in its 3′ was obtained by PCR using the 5′-GGATCCTTTCTTCACA-CAGCTTGGCCA-3′ and 5′-CTATTTCTTCACACAGCTTGGCCA-TGT-3′ oligonucleotides, and cloned in the pCR3.1-Uni vector (CLONTECH Laboratories, Inc.). Ratiometric pHLuorin was then cloned in the BamHI-EcoRI sites. Nter-TIVAMP, Cyt-TIVAMP, and coiled-coiled domain of TIVAMP (CC-TIVAMP; from E^{119} to K^{188}) were fused to GST gene by cloning in pGEX4T vector (Amersham Pharmacia Biotech).

Overlay Assay

The corresponding GST fusion proteins and GST alone were produced and purified as described (Galli et al., 1998). $6\times$his-tagged SNAP25A ($6\times$hisSNAP25, bacterial strain was a generous gift from G. Schiavo, ICRF, London, UK) was purified as described (Weber et al., 1998). $6\times$hisSNAP25 was run on SDS-PAGE and Western blotted onto Immobilon-P membrane (Millipore). The amount of 6xhisSNAP25 corresponds to 1.25 μg/mm of membrane. 4-mm strips of the membrane were cut and incubated in 150 mM NaCl, 5% nonfat dry milk, 50 mM phosphate, pH 7.5, for buffer for 1 h at room temperature. The strips were then incubated with 10 nM of the GST fusion proteins overnight at 4°C in buffer B (3% BSA, 0.1% Tween 20, 20 mM Tris, pH 7.5) containing 1 mM DTT. The strips were rinsed three times in buffer B at room temperature, incubated with anti-GST antibodies in buffer B for 1 h, rinsed in buffer B three times and incubated with alkaline phosphatase-coupled sheep anti–mouse antibodies. The detection was carried out simultaneously for all the strips, for the same time, using a kit from Promega.

Cell Transfection

PC12 or HeLa cells were trypsinized, washed, and resuspended at a density of 7.5–10 $\times$ 10^6 cells/ml in Optimix (Equibio). Electroporation was performed with 10 μg DNA in a final volume of 0.8 ml cell suspension using a Gene Pulser II device (Bio-Rad) with one shock at 950 μF and 250 V. When GFP was cotransfected with TeNT or BoNTE for monitoring the transfected cells, the plasmid carrying the GFP gene was added at double concentration in order to ensure that all the cells that uptake it also uptake the plasmid carrying the toxin. Immediately after electroporation, cells were washed with 5 ml of complete medium before plating them for immunoprecipitation or immunofluorescence microscopy analysis. 5 h later, the outgrowth medium was removed and replaced with fresh medium containing 100 nM staurosporine (Sigma-Aldrich). PC12 and HeLa cells were processed 24 or 48 h after transfection, respectively. For enhanced expression of the exogenous proteins, 5 mM sodium butyrate was added in all the cases during the last 6 h before processing the cells.

Antibody Uptake Assay

PC12 cells processed as indicated above were incubated in the presence of 5 μg/ml anti-GFP antibody in culture medium for 15 min on ice, 15 min on ice then 15 min at 37°C, or 15 min on ice then 60 min at 37°C, 24 h after transfection with GFP-TIVAMP or TIVAMP-GFP. The cells were then washed twice with culture medium and twice with PBS, fixed with PFA, and processed for immunofluorescence.

Immunocytochemistry

Cells were fixed with 4% PFA and processed for immunofluorescence as previously described (Coco et al., 1999). Optical conventional microscopy was performed on a Leica microscope equipped with a MicroMax CCD camera (Princeton Instruments). Confocal laser scanning microscopy was performed using a TCS confocal microscope (Leica). Images were assembled without modification using Adobe Photoshop.

Neurite Outgrowth Assay

Cells were fixed 24 h after transfection. Between 20 and 100 randomly chosen fields for each condition were taken with a MicroMax CCD camera (Princeton Instruments), resulting in the analysis of at least 50 GFP-positive cells. A neurite was defined as a thin process longer than 5 μm. Using the Metamorph software (Princeton Instruments) two parameters were scored in each case: the number of neurites per cell (from 0 to 4 or more neurites), and the length of each neurite, from the cell body limit until the tip of the process. The obtained data were analyzed for their statistical significance with SigmaStat (SPSS, Inc.). All the recordings and the Metamorph analysis were done in blind.

Videomicroscopy

Living PC12 cells transfected and treated with staurosporine as described above were placed in complete medium in an appropriate chamber equilibrated at 37°C and 5% CO_2. Cells were monitored with a MicroMax CCD camera (Princeton Instruments) for as much as 9 h, taking images both through phase contrast and FITC fluorescence every 2 min or every 15 s. Images were assembled using Metamorph (Princeton Instruments).

Immunoprecipitation

Immunoprecipitation from rat brain was performed using a Triton X-100–soluble membrane fraction prepared as follows: two adult rat brains were homogenized with a glass/teflon homogenizer (9 strokes at 900 rpm) in 25 ml of 0.32 M sucrose containing a protease inhibitor cocktail. All the steps were carried out at 4°C. After 10 min centrifugation at 800 g the supernatant was centrifuged at 184,000 g for 1 h, obtaining a cytosolic and a membrane fraction in the supernatant and the pellet, respectively. The pellet was resuspended in TSE (50 mM Tris, pH 8.0, 0.5 mM EDTA, and 150 mM NaCl) containing 1% Triton X-100 for 30 min and finally the insoluble material was removed by centrifugation at 184,000 g for 1 h. Immunoprecipitation with anti-SNAP25 antibodies and mouse control IgGs was performed from 2 mg of proteins from the soluble extract. Immunoprecipitations from transfected PC12 or HeLa cells were performed using a total Triton X-100–soluble fraction prepared as follows: after two washes with cold TSE, cells were lysed for 1 h under continuous shaking with TSE containing 1% Triton X-100 and protease inhibitors. The supernatant resulting from centrifugation at 20,000 g for 30 min was used for immunoprecipitation. After overnight incubation of the brain and cell extracts with the antibodies, 50 μl of magnetic beads (Dynabeads; Dynal) were added for 2–4 h. The magnetic beads were washed four times with TSE containing 1% Triton X-100, eluted with gel sample buffer and the eluates were boiled for 5 min and run on SDS-PAGE gels (Schagger and von Jagow, 1987).

Online Supplemental Material

To better visualize GFP-TIVAMP dynamics in staurosporine-differentiated PC12 cells, we advise the reader to consult the supplementary video available online at http://www.jcb.org/cgi/content/full/149/4/889/DC1. This video corresponds to the same GFP-TIVAMP–expressing cell as presented in Fig. 2, shown here during a longer period of time (6 h), with images taken every 2 min (8 images/s). The movie shows the dynamics of GFP-TIVAMP (bottom) in the course of neurite outgrowth (as seen by transmission light [TL], top). Note that most movements of GFP-TIVAMP–containing vesicles are anterograde.

Results

TI-VAMP Dynamics in Staurosporine-treated PC12 Cells

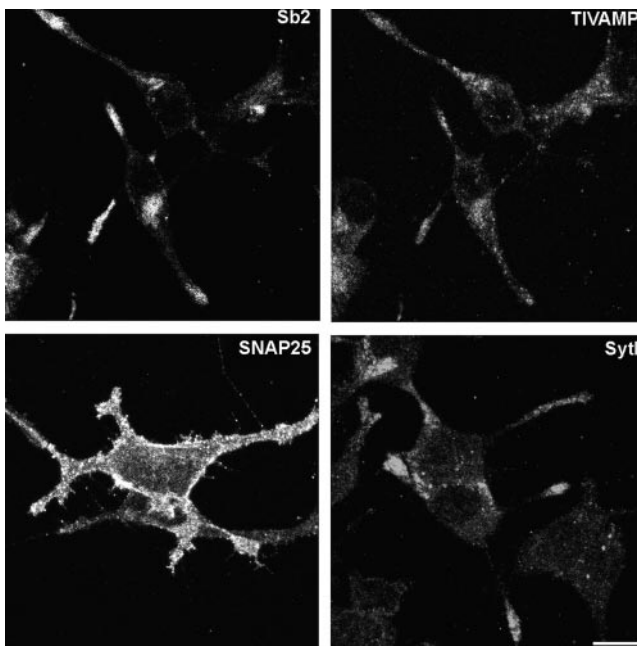Differentiation of neurons and nerve growth factor (NGF)-

Figure 1. Localization of membrane markers in horizontal confocal sections of staurosporine-differentiated PC12 cells. PC12 cells were treated with 100 nM staurosporine for 24 h, fixed and processed for immunofluorescence with anti-synaptobrevin 2 (Sb2) and anti–TI-VAMP (TIVAMP), anti-SNAP25 (SNAP25) or anti-synaptotagmin I (Syt I) antibodies. The cells were then observed by confocal microscopy. Note the lack of colocalization of synaptobrevin 2 and TI-VAMP, the restricted localization of SNAP25 at the plasma membrane and the concentration of synaptotagmin I at the tip of neurites. Bar, 5 μm.

induced neurite outgrowth of PC12 cells take several days (Luckenbill-Edds et al., 1979). On the contrary, staurosporine, a protein kinase inhibitor, induces maximal neurite outgrowth in 24 h of treatment in PC12 cells (Yao et al., 1997). Our neurite outgrowth assay is based on treating PC12 cells with 100 nM staurosporine for 24 h. These experimental conditions do not induce apoptosis in PC12 cells (Yao et al., 1997; Li et al., 1999). Fig. 1 shows that synaptobrevin 2, TI-VAMP, SNAP25, and synaptotagmin I had a normal subcellular localization in staurosporine-treated PC12 cells (Fig. 1). Synaptobrevin 2 concentrated in the perinuclear region and in neuritic tips. TI-VAMP–positive vesicles were scattered throughout the cytoplasm and concentrated at the leading edge of extending neurites. Synaptotagmin I appeared almost exclusively in neurites and varicosities and SNAP25 was present throughout the plasma membrane. This pattern of immunostaining was similar to that observed in NGF-treated PC12 cells (Chilcote et al., 1995; Coco et al., 1999), demonstrating the validity of this cellular model to study neurite outgrowth.

We produced TI-VAMP carrying a GFP tag fused to the NH_2-terminal end (GFP-TIVAMP, see Fig. 4 B). Upon transfection of this construct in PC12 cells, GFP staining was indistinguishable from that of endogenous TI-VAMP by confocal microscopy (data not shown), thus discarding the possibility that fusion of the GFP tag could alter TI-VAMP trafficking. We then observed TI-VAMP dynamics by time-lapsed videomicroscopy in staurosporine-treated
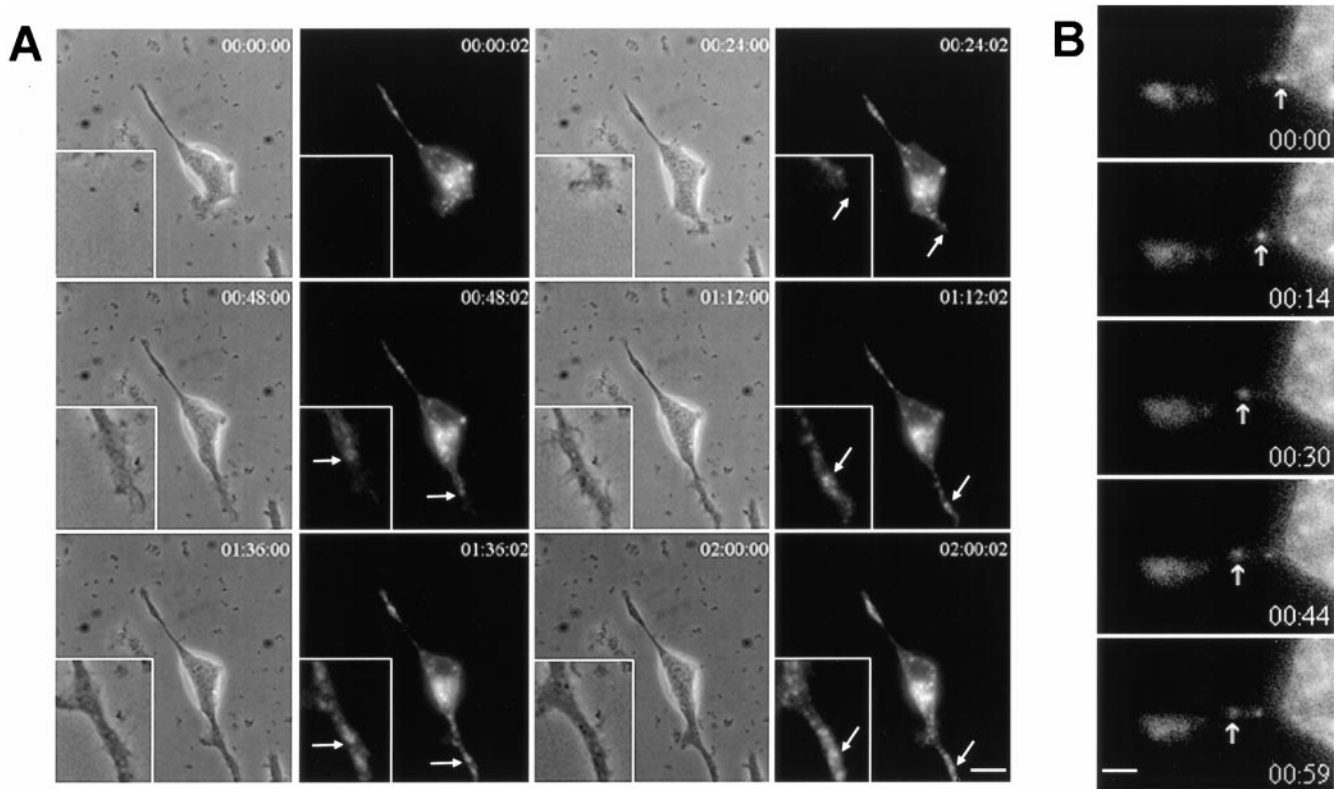
Figure 2. Dynamics of GFP-TIVAMP-vesicles. PC12 cells transfected with GFP-TIVAMP were treated with staurosporine for 5 h and observed under time-lapsed videomicroscopy in the presence of staurosporine. (A) GFP-TIVAMP vesicles accompany the growth of neurites. Transmission and fluorescent light images were recorded every 2 min over a period of 8 h. Images recorded every 24 min through the middle period of the whole recording are shown (see also movie). The inset shows a higher magnification of a growing neurite. Arrows indicate regions of this neurite where GFP-TIVAMP concentrates. (B) GFP-TIVAMP vesicles dynamics in neurites. Fluorescent light images were recorded every 15 s over a period of 30 min (bottom right number, time in s). Images recorded during a 1-min period of the recording are shown. The arrow indicates a GFP-TIVAMP vesicle which is moving anterogradely. See supplemental video at http://www.jcb.org/cgi/content/full/149/4/889/DC1. Bars: (A) 5 μm; (B) 1 μm.

PC12 cells, which had been previously transfected with GFP-TIVAMP (Fig. 2). Fast growing neurites were recorded every 2 min over periods of 3–9 h, 5 h after the onset of staurosporine treatment. Fig. 2 A displays transmission and fluorescent light images recorded every 24 min during 2 h 2 min (see also accompanying movie). High magnification view of a neurite growing towards the bottom right of the image is shown in the inset. At each time point, GFP-TIVAMP–containing vesicles distributed along this growing process, up to the leading edge of the growth cone (Fig. 2 A). Most movements of GFP-TIVAMP–containing membranes were anterograde (Fig. 2 B).

We then constructed another form of fluorescent TI-VAMP by introducing a GFP tag at the COOH terminus (TIVAMP-GFP, see Fig. 4 B). In this case, the GFP tag is exposed to the extracellular medium after exocytosis of TI-VAMP–containing vesicles. TIVAMP-GFP–transfected PC12 cells were labeled with monoclonal antibodies directed against GFP while they were placed on ice, before fixation. The labeling was often concentrated at the tip of the growing neurite (Fig. 3). When the cells were allowed to internalize the antibody at 37°C, we observed a fast, time-dependent uptake. After 15 min at 37°C, the anti-GFP immunoreactivity was seen in peripheral structures,

very close to the plasma membrane with a low degree of overlap with the green signal emitted by the bulk of TIVAMP-GFP. After 60 min, most of the immunoreactivity colocalized with TIVAMP-GFP, indicating that the anti-GFP antibody had reached the entire TIVAMP-GFP compartment. We did not detect any plasma membrane labeling nor GFP antibody internalization in GFP-TIVAMP–transfected or untransfected cells (Fig. 3) thus demonstrating the lack of capture of the antibody by fluid phase uptake. Altogether, these studies demonstrate that the dynamics of TI-VAMP–containing vesicles very closely accompany the growth of neurites and that the protein recycles at the neuritic plasma membrane.

The NH₂-terminal Domain of TI-VAMP Inhibits SNARE Complex Formation

Because TI-VAMP is resistant to NT treatment, new experimental approaches had to be developed to study its function in living cells. Towards this goal, we searched for mutated forms of TI-VAMP that would have impaired SNARE complex formation activity. We first identified SNAP25 as a main physiological target SNARE (t-SNARE) of TI-VAMP. SNAP25, a neuronal plasma membrane
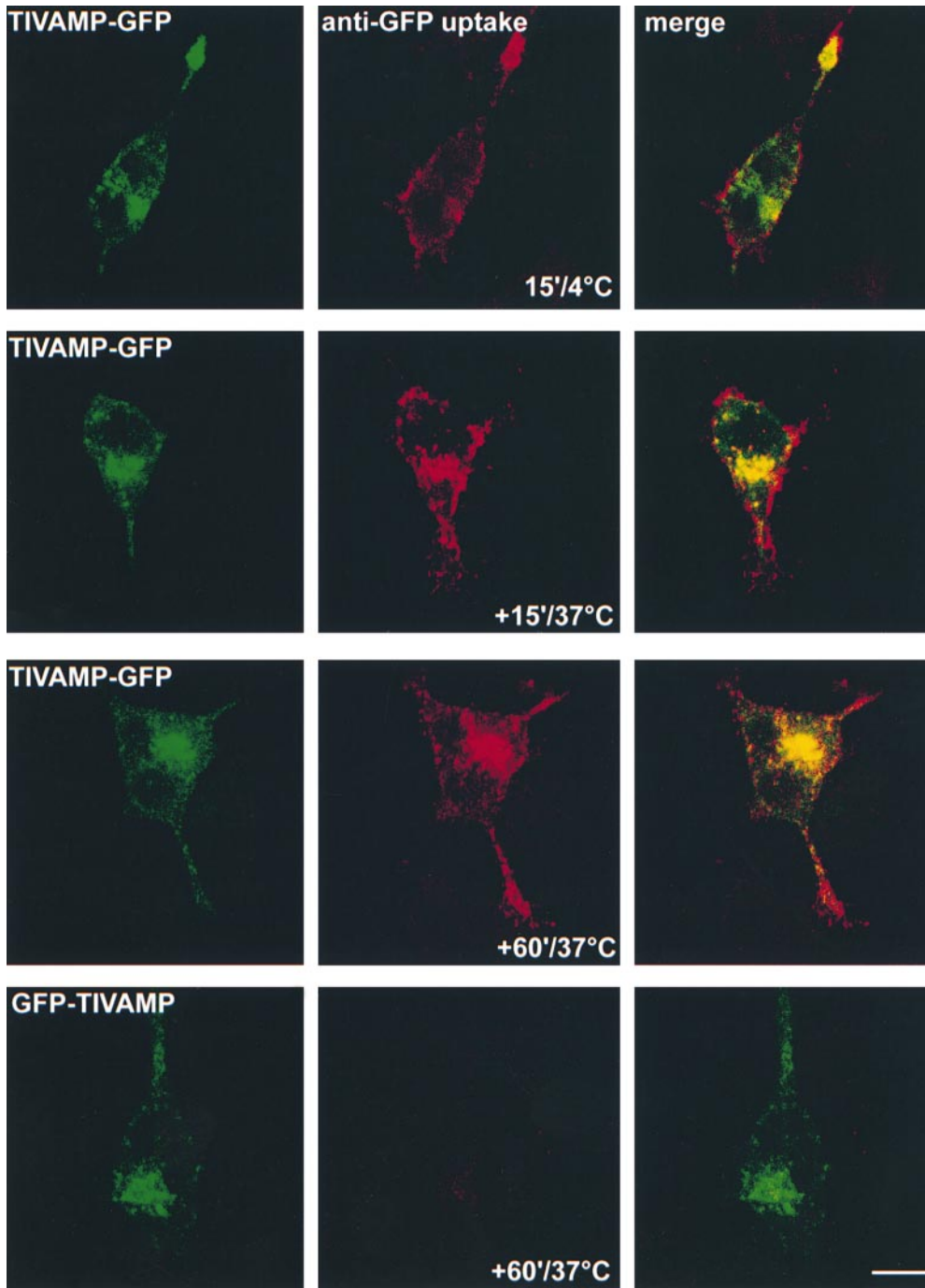
Figure 3. TI-VAMP recycles at the neuritic plasma membrane. PC12 cells transfected with TIVAMP-GFP or GFP-TIVAMP and treated with staurosporine for 20 h were placed on ice, incubated with monoclonal antibody anti-GFP (5 μg/ml) for 15 min, and directly fixed (15′/4°C) or further incubated at 37°C for 15 min (+15′/37°C) or 60 min (+60′/37°C) before fixation. Note the dense labeling of the neuritic plasma membrane in the 15′/4°C and +15′/37°C conditions. Full loading of the GFP-TIVAMP compartment is reached in the +60′/37°C condition. Bar, 5 μm.

Q-SNARE, formed abundant SNARE complexes with TI-VAMP as seen by coimmunoprecipitation experiments performed from brain extracts. Cellubrevin, a v-SNARE that is expressed in glial cells but not in neurons (Chilcote et al., 1995), did not associate with SNAP25 thus showing that the SNARE complexes were not formed during solubilization of brain membranes (Fig. 4 A).

Protein sequence analysis of TI-VAMP shows that the protein has an original NH_2-terminal (Nter) domain of 120 amino acids, located upstream of the coiled-coiled domain (also called R-SNARE motif; Galli et al., 1998; Jahn and Sudhof, 1999). This Nter domain includes three regions predicted to be α helical by Hydrophobic Cluster Analysis (Callebaut et al., 1997) and Jpred (Cuff et al., 1998; data not shown). This is reminiscent of the Nter domain of syntaxin 1, which comprises 3 α helices (Fernandez et al., 1998) and inhibits lipid bilayer fusion (Parlati et al., 1999). The Nter domain of Sso1p, the yeast homologue of syntaxin 1, inhibits the rate of SNARE complex formation (Nicholson et al., 1998). Similar Nter domains are present in the other plasma membrane but not in intracellular syntaxins (Fernandez et al., 1998), indicating that this function may be specific for exocytosis. This led us to prepare the following GST fusion proteins: full cytoplasmic domain of TI-VAMP (GST-Cyt-TIVAMP), coiled-coiled domain alone (GST-CC-TIVAMP), and Nter domain alone (GST-
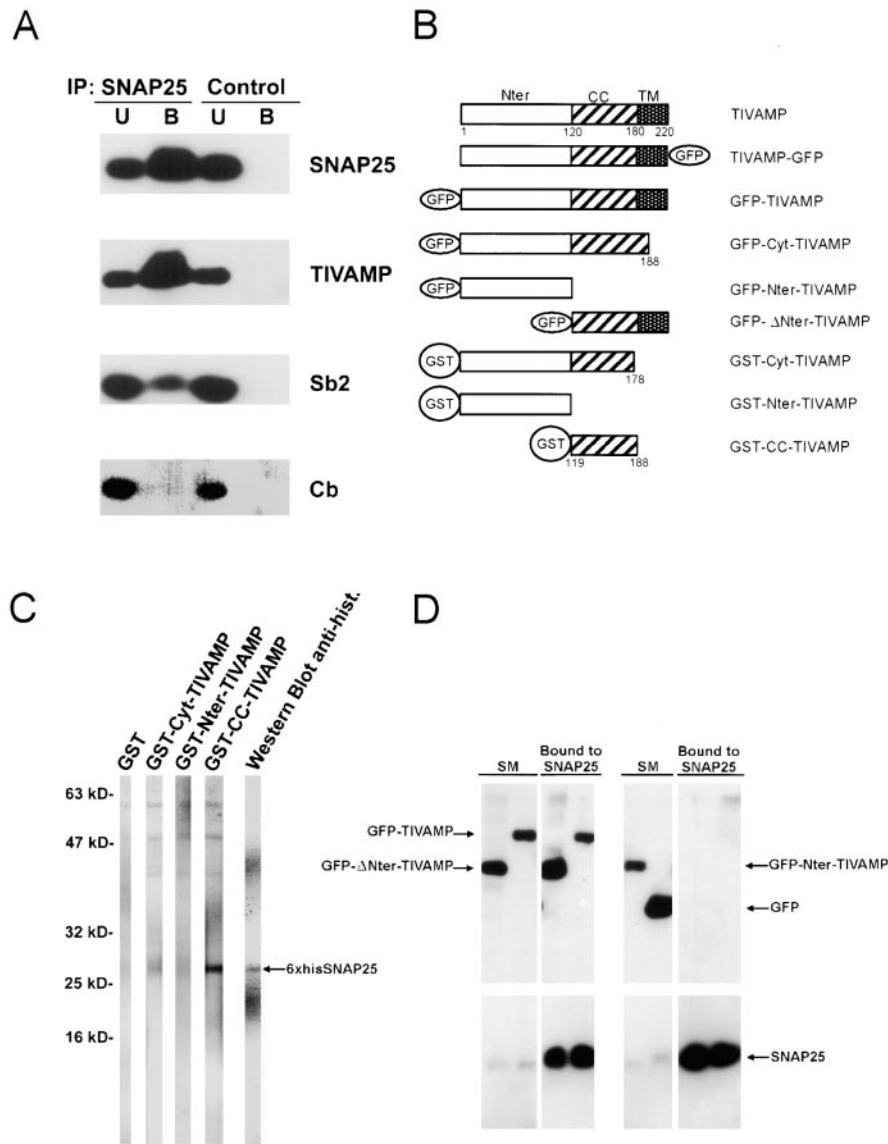
A

IP: SNAP25   Control
   U   B   U   B

SNAP25

TIVAMP

Sb2

Cb

B

C

D

Figure 4. Biochemical properties of the TI-VAMP–SNAP25 complex. (A) TI-VAMP forms a complex with SNAP25 in Triton X-100 extract of rat brain. Immunoprecipitation with anti-SNAP25 antibodies was performed from Triton X-100–soluble extract of rat brain as described in Materials and Methods and immunoprecipitated proteins were detected by Western blot analysis with the indicated antibodies (Sb2, synaptobrevin 2; Cb, cellubrevin; U, unbound; B, bound to anti-SNAP25 immunobeads). The bound fraction corresponded to a 65-fold enrichment compared with unbound. The SNAP25–TI-VAMP complex seemed more abundant than the SNAP25–synaptobrevin 2 complex but this may only reflect a lower expression level of TI-VAMP compared with synaptobrevin 2 in the adult brain. Note that cellubrevin did not coimmunoprecipitate with SNAP25. (B) Structure of TI-VAMP and TIVAMP–derived constructs. TI-VAMP is composed of three domains: the Nter domain (amino acids 1–120), the coiled-coiled domain, also called R-SNARE motif (CC, amino acids 121–180), and one comprising the transmembrane domain and a short luminal domain (TM, amino acids 181 to 220). These domains were tagged with GFP and GST as depicted. (C) The Nter domain of TI-VAMP inhibits binding of TI-VAMP to SNAP25. The binding of GST, GST-Cyt-TIVAMP, GST-Nter-TIVAMP, or GST-CC-TIVAMP was measured by overlay over immobilized 6×his-SNAP25 (indicated by the arrow). GST-CC-TIVAMP bound efficiently to immobilized 6×his-SNAP25. Little binding of GST-Cyt-TIVAMP and none of GST and GST-Nter-TIVAMP was observed. As positive control, a strip was revealed with anti-6×histidine antibodies. (D) A TI-VAMP mutant lacking the Nter domain coimmunoprecipitates with SNAP25 more efficiently than full-length TI-VAMP. HeLa cells cotransfected with SNAP25 plus GFP-ΔNter-TIVAMP, GFP-TIVAMP, GFP-Nter-TIVAMP, or GFP were lysed and subjected to immunoprecipitation with mouse monoclonal anti-SNAP25 antibodies as described in Materials and Methods. The immunoprecipitated proteins were then detected by Western blot with anti-GFP or anti-SNAP25 rabbit polyclonal antibodies. The bound fraction corresponded to a 100-fold enrichment compared with the starting material (SM) in the case of the GFP blot and to a 10-fold enrichment in the case of the SNAP25 blot. Note that neither GFP-Nter-TIVAMP nor GFP coimmunoprecipitated with SNAP25.

Nter-TIVAMP; Fig. 4 B), and to measure the binding of the corresponding proteins to immobilized 6xhis-SNAP25 in an overlay assay. GST-CC-TIVAMP bound very efficiently immobilized his-SNAP25 whereas GST-Cyt-TIVAMP bound very poorly. As controls, GST alone and GST-Nter-TIVAMP did not bind immobilized his-SNAP25 (Fig. 4 C). To perform in vivo experiments, we constructed the following GFP-tagged forms of TI-VAMP: TI-VAMP deleted of its Nter domain (GFP-ΔNter-TIVAMP) and Nter domain alone (GFP-Nter-TIVAMP; Fig. 4 B). HeLa cells do not express endogenous SNAP25, so we used them to study the association of SNAP25 with GFP-TIVAMP, GFP-ΔNter-TIVAMP, GFP-Nter-TIVAMP (Fig. 4 B), or GFP, in vivo, after

cotransfection. We measured the amount of GFP-tagged proteins coimmunoprecipitating with SNAP25 from Triton X-100–soluble extracts. GFP-ΔNter-TIVAMP formed more abundant SNAP25-containing SNARE complexes than GFP-TIVAMP. As controls, GFP and GFP-Nter-TIVAMP did not bind SNAP25 (Fig. 4 D). Altogether, we propose that the Nter domain exerts an intramolecular inhibition of the SNARE complex formation activity of TI-VAMP's coiled-coiled domain.
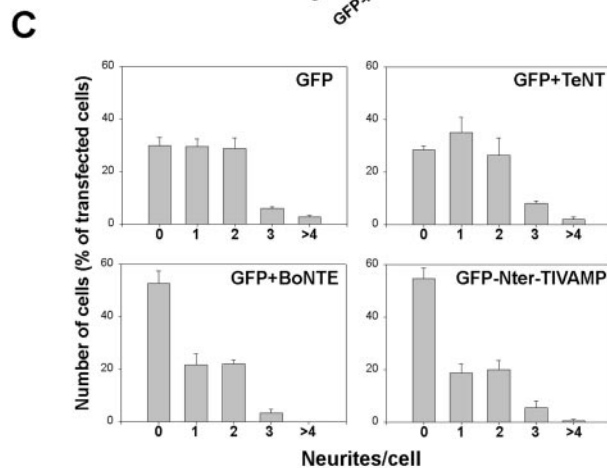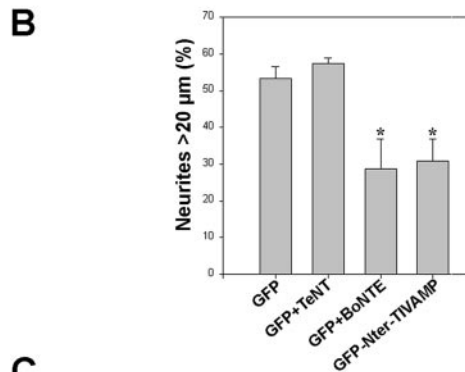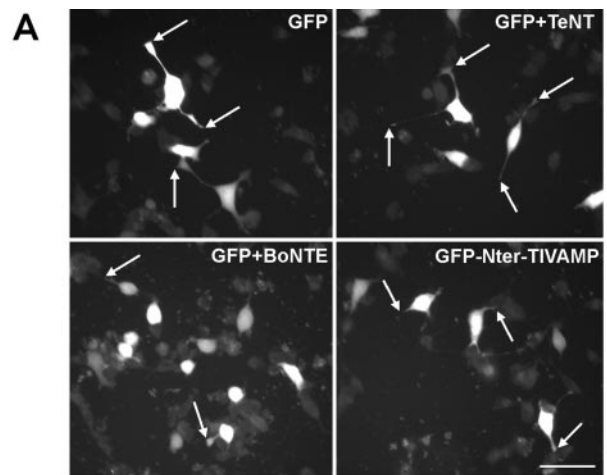
TI-VAMP Mediates Neurite Outgrowth

An assay was set up to measure the effect of transfection of NTs and TI-VAMP mutants on staurosporine-induced

neurite outgrowth in PC12 cells. First, we showed that when cells were electroporated with two plasmids, virtually all cells expressed both transgenes. This was demonstrated by transfection with GFP-cellubrevin (GFP-Cb) alone, TeNT alone, or both. Cotransfection of TeNT with GFP-Cb resulted in total proteolysis of GFP-Cb (not shown). Second, the activities of transfected TeNT and BoNT E were demonstrated by complete proteolysis of endogenous synaptobrevin 2 and SNAP25, respectively (not shown).

In a first set of experiments, PC12 cells were transfected with GFP alone, GFP plus TeNT, GFP plus BoNT E or GFP-Nter-TIVAMP. The cells were then treated with staurosporine and fixed after 24 h. Fig. 5 A shows a representative field observed in each condition. Neurites from cells transfected with GFP or GFP plus TeNT were similar to neurites from untransfected cells. Neurites from cells transfected with GFP plus BoNT E or GFP-Nter-TIVAMP were fewer and shorter. The length of neurites and the number of neurites per cell were measured in each GFP-positive cell, in each condition. GFP plus TeNT had no effect on neurite number and length compared with GFP alone. BoNT E reduced by 45% the number of neurites longer than 20 μm and strongly increased the number of cells without neurites (Fig. 5, B and C). Expression of the Nter domain of TI-VAMP had an effect that was similar to that of BoNT E. GFP-Nter-TIVAMP reduced by 42% the number of neurites longer than 20 μm and strongly increased the number of cells without neurites (Fig. 5, B and C). The effects of GFP plus BoNT E and GFP-Nter-TIVAMP were statistically different from GFP alone with $P = 0.027$ and 0.017 (Student's t test), respectively. The effects of BoNT E and GFP-Nter-TIVAMP were not additive (not shown), indicating that they act on the same exocytotic mechanism. In a different set of experiments, we measured the effect of GFP and the cytoplasmic domain (Nter and coiled-coiled domains) of TI-VAMP fused to GFP (GFP-Cyt-TIVAMP, Fig. 4 B). GFP-Cyt-TIVAMP (neurites longer than 20 μm: 50.2% $\pm$ 0.25) had no effect on neurite length compared with GFP (neurites longer than 20 μm: 50.7% $\pm$ 3.5). GFP-Cyt-TIVAMP had no effect on the number of neurites per cell (not shown). These results demonstrated that neurite outgrowth in staurosporine-treated cells is insensitive to TeNT but sensitive to BoNT E as in neurons. The fact that GFP-Nter-TIVAMP inhibited neurite outgrowth as strongly as BoNT E suggests that TI-VAMP plays a major role in neurite outgrowth.

We then checked that GFP-Nter-TIVAMP expression did not have a deleterious effect. Fig. 6 shows a gallery of double immunofluorescence experiments performed in GFP-Nter-TIVAMP–transfected cells. We observed no ef-

Figure 5. Expression of the Nter domain of TIVAMP inhibits neurite outgrowth. (A) Effect of GFP, GFP plus TeNT, GFP plus BoNT E, or GFP-Nter-TIVAMP on neurite outgrowth. PC12 cells transfected with the indicated constructions and treated with staurosporine were fixed and direct fluorescence images were recorded. Representative fields of the distinct phenotypes found are shown. Note the long neurites displayed both by the GFP and the GFP+TeNT–transfected cells compared with the shorter ones displayed by the GFP+BoNT E and the GFP-Nter-TIVAMP-transfected cells (arrowheads). (B) GFP-Nter-TIVAMP and BoNT E inhibit neurite length. Percentage of neurites longer than 20 μm. A minimum of 50 transfected cells of each type was recorded in blind, and the length of all their neurites was measured. The mean values ($\pm$SE) of percentage of neurites longer than 20 μm from three independent experiments are shown. *$P < 0.03$ (Student's t test). Note the lack of effect of TeNT and that BoNT E and GFP-Nter-TIVAMP had a similar inhibitory effect on neurite length. (C) Number of neurites per cell. The same randomly chosen transfected cells were use to quantify the number of neurites per cell. Shown is the number of cells, expressed as the percentage of transfected cells, displaying 1, 2, 3, or > 4 neurites. The mean values ($\pm$SE) of three independent experiments are shown. Note the lack of effect of TeNT and that both BoNT E and GFP-Nter-TIVAMP enhanced the percentage of cells without neurites. Bar, 25 μm.
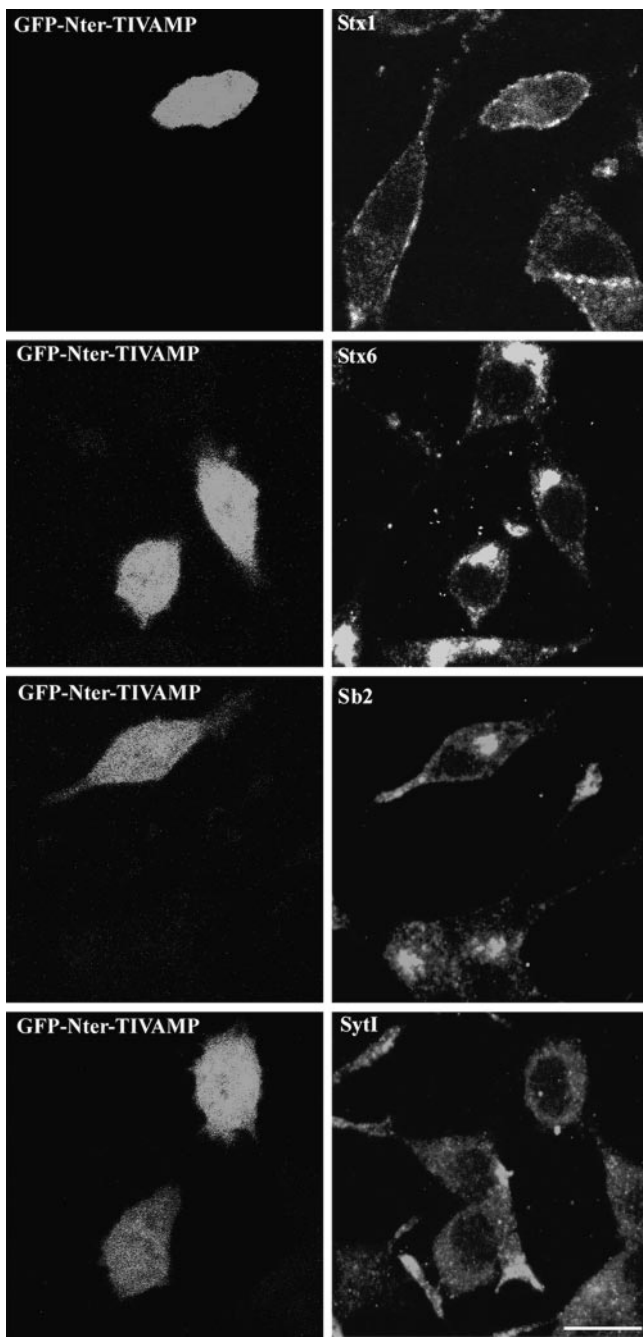
Figure 6. Morphology of GFP-Nter-TIVAMP–expressing cells. PC12 cells transfected with GFP-Nter-TIVAMP and treated with staurosporine as in Fig. 5 were fixed, processed for double fluorescence by combining direct GFP fluorescence detection with indirect immunofluorescence detection using the indicated antibodies. Representative GFP-Nter-TIVAMP–transfected cells without or with short neurite(s) are shown in horizontal confocal sections. Syntaxin (Stx) 1 and 6 and synaptobrevin 2 (Sb2) have a localization similar in untransfected as in GFP-Nter-TIVAMP–expressing cells. Synaptotagmin I immunoreactivity was weaker in GFP-Nter-TIVAMP–transfected cells than in untransfected cells. Bar, 10 μm.

fect on the localization of syntaxin 1, a plasma membrane SNARE, syntaxin 6, a Golgi apparatus SNARE (Fig. 6), and SNAP25 (not shown) when compared with untransfected or GFP-transfected cells. Synaptobrevin 2 appeared

both in the perinuclear region and in the shorter neurites emerging from GFP-Nter-TIVAMP cells (Fig. 6 and compare with Fig. 1). These cells showed a lower level of expression of synaptotagmin I. Synaptotagmin I was the vesicular marker which was the most enriched in the tip of the neurites in untransfected cells (Figs. 1 and 6) so our result may suggest that synaptotagmin I reached the neuritic tip by a TI-VAMP–dependent pathway. These results showed that the Nter domain of TI-VAMP had a specific inhibitory effect on neurite outgrowth.

We then tested the effect of GFP-ΔNter-TIVAMP expression and compared it with that of GFP-TIVAMP on neurite outgrowth. We observed the occurrence of unusually long neurites with an increased number of filopodia. Staining of actin filaments with fluorescent phalloidin showed that the neurites of GFP-ΔNter-TIVAMP–transfected cells showed cortical actin localization similar to GFP-TIVAMP–transfected cells (Fig. 7 A). The pattern of staining of tubulin, synaptobrevin 2, synaptotagmin I, SNAP25, and syntaxin 1 was the same in GFP-ΔNter-TIVAMP as in GFP-TIVAMP–transfected and in untransfected cells (data not shown). The effect of GFP-ΔNter-TIVAMP was quantified as in the case of GFP-Nter-TIVAMP. GFP-ΔNter-TIVAMP expression doubled the number of neurites longer than 30 μm and multiplied by 5 the number of neurites longer than 50 μm when compared with the expression of GFP-TIVAMP (Fig. 7 B). GFP-TIVAMP had no effect on neurite length and number per cell compared with GFP alone (not shown). We observed no effect of GFP-ΔNter-TIVAMP on the number of neurites per cell (not shown). We checked that GFP-ΔNter-TIVAMP formed more abundant SNARE complexes with endogenous SNAP25 by measuring the amount of SNAP25 and syntaxin 1 that was coimmunoprecipitated with GFP-ΔNter-TIVAMP, GFP-TIVAMP, and GFP-Sb2. GFP-ΔNter-TIVAMP–SNAP25 complex was 2.5 times more abundant than GFP-TIVAMP–SNAP25. Accordingly, GFP-ΔNter-TIVAMP coimmunoprecipitated more syntaxin 1 than GFP-TIVAMP (Fig. 7 C). These results showed that a form of TI-VAMP, which had a higher SNARE complex formation activity, strongly enhanced neurite outgrowth.

Discussion

This study demonstrates that TI-VAMP–mediated vesicular transport is essential for neurite outgrowth. Expression of the NH$_2$-terminal domain of TI-VAMP inhibits neurite outgrowth as strongly as BoNT E, which abolishes the expression of SNAP25, a plasma membrane SNARE partner of TI-VAMP. On the contrary, activation of neurite outgrowth and increased SNARE complex formation were observed when the NH$_2$ terminus deletion mutant of TI-VAMP was expressed in PC12 cells.

A main conclusion from our work is that TI-VAMP is involved in neurite outgrowth in PC12 cells. Our finding that TI-VAMP interacts with SNAP25 in PC12 cells and in the brain is consistent with the involvement of SNAP25 in neurite outgrowth (Osen-Sand et al., 1993, 1996). The TI-VAMP–dependent vesicular transport mediating neurite outgrowth in PC12 cells likely corresponds to the outgrowth of axons and dendrites in developing neurons. In-
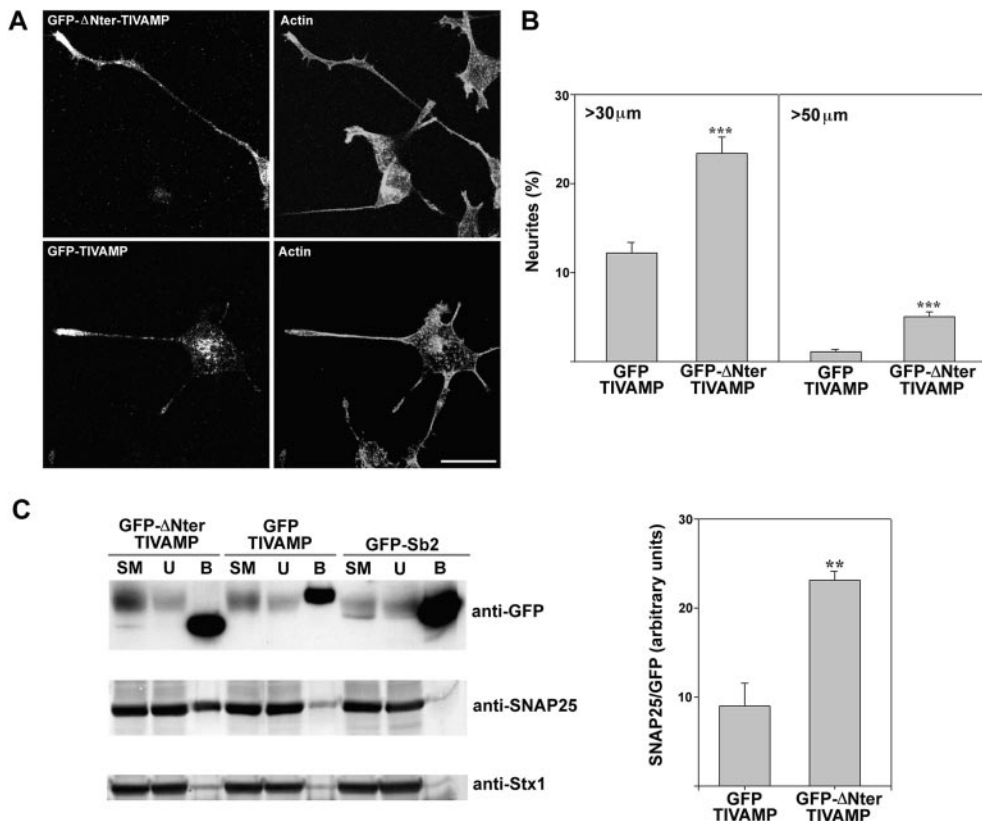
Figure 7. Expression of a TIVAMP mutant lacking the NH$_2$-terminal domain enhances neurite outgrowth. (A) Morphology of PC12 cells transfected with GFP-TIVAMP or GFP-ΔNter-TIVAMP. The cells were transfected, treated with staurosporine as in Fig. 5, fixed/permeabilized, and processed for double fluorescence by combining direct GFP fluorescence detection with indirect immunofluorescence detection using Texas red–phalloidin to visualize the actin filaments. Note the occurrence of numerous filopodia in the neuritic tip of the GFP-ΔNter-TIVAMP–transfected cell. (B) GFP-ΔNter-TIVAMP increases neurite length. A minimum of 100 transfected cells of each type was recorded in blind, and the length of all their neurites was measured. The mean values (±SE) of the percentage of neurites longer than 30 or 50 μm from three independent experiments is shown. *** Indicates $P < 0.001$ (Student's t test). (C) GFP-ΔNter-TIVAMP enhances formation of SNARE complexes. A Triton X-100–soluble extract was prepared from PC12 cells transfected with GFP-TIVAMP, GFP-ΔNter-TIVAMP, or GFP-Sb2 and subjected to overnight immunoprecipitation with monoclonal anti-GFP antibodies. Immunoprecipitated proteins were resolved in SDS-PAGE followed by Western blot analysis with the indicated antibodies. Note the increased coimmunoprecipitation of endogenous SNAP25 with GFP-ΔNter-TIVAMP compared with GFP-TIVAMP. The histogram in the right side shows the quantification of the amount of endogenous SNAP25 immunoprecipitated normalized to the amount of GFP fusion protein immunoprecipitated from two independent experiments. **$P < 0.01$ (Student's t test). Bar, 10 μm.

deed, TI-VAMP concentrates in the leading edge of axonal and dendritic growth cones of hippocampal neurons in primary culture (Coco et al., 1999). In support of this conclusion, preliminary experiments have shown a decreased number of neurites in young hippocampal neurons, which were microinjected with anti-TIVAMP antibodies (Coco, S., M. Matteoli, and T. Galli, unpublished observations). Neurite outgrowth may be also very active in differentiated neurons because it may participate to post-synaptic morphological changes related to plasticity and learning (MaleticSavatic et al., 1999). A role for SNAP25 in neuronal plasticity and learning has been proposed (Catsicas et al., 1994; Boschert et al., 1996). Therefore, the TI-VAMP– and SNAP25-dependent vesicular transport mechanism described here could also mediate activity-dependent exocytosis involved in dendrite elongation and post-synaptic receptor expression at the plasma membrane in mature neurons (MaleticSavatic et al., 1999; Noel et al., 1999; Shi et al., 1999). This could account for the distribution of TI-VAMP–containing vesicles throughout the dendrites (Coco et al., 1999) and of SNAP25 in the dendritic plasma membrane (Galli et al., 1995; Garcia et al., 1995) of mature neurons.

In a previous study, we proposed that TI-VAMP defines a novel tubulovesicular compartment, which excludes SV and endosomal markers, partially overlaps with CD63 and could correspond to a constitutive-like secretory compartment in neuronal cells (Coco et al., 1999). Interestingly, CD63 was recently found in Weibel-Palade bodies, which secrete von Willebrand factor and transport P-selectin, in endothelial cells (Kobayashi et al., 2000). In fibroblasts, TI-VAMP partially overlaps with lysosome-associated membrane protein 1 (LAMP1) and antibodies against TI-VAMP inhibit the degradation of EGF (Advani et al., 1999). These findings together with the present data showing that TI-VAMP mediates neurite outgrowth could be in favor of the involvement of TI-VAMP in constitutive-like secretion in neurons, a pathway related to secretory lysosomes in non-neuronal cells. Indeed, some of the constitutive secretory proteins are targeted to immature secretory granules in neuronal cells. Then, they are removed from maturing granules and sent to immature secretory granule-derived vesicles, together with lysosomal enzymes. Immature secretory granule-derived vesicles reach the plasma membrane and release their content in the extracellular medium thus defining a constitutive-like secretory pathway in neuronal cells (Thiele et al., 1997). Future studies should aim to determine which cargo proteins and

lipids TI-VAMP–containing vesicles transport in neurons. According to our working hypothesis, the proteic and lipidic map of TI-VAMP vesicular compartment is likely to identify factors, which are important for neurite elongation both in developing and mature neurons. The purification of TI-VAMP vesicular compartment will also be important to determine which other proteins are involved in this pathway, particularly rab proteins that have been shown to play a role in neurite outgrowth (Ayala et al., 1990; Huber et al., 1995).

The mechanism of action of the NH_2-terminal domain of TI-VAMP has not been yet fully resolved but it is reminiscent of the inhibitory effects of NH_2-terminal domains of Sso1p and syntaxin 1. NH_2-terminal deletion mutant of Sso1p has an increased SNARE complex formation rate. The NH_2-terminal domain of Sso1p binds to its SNARE motif and inhibits SNARE complex formation in vitro, thus acting as an intramolecular inhibitor of the SNARE motif (Nicholson et al., 1998). Removal of the NH_2-terminal domain of syntaxin 1 decreases SNARE-dependent liposome fusion half time from 40 to 10 min. In this case, no effect is observed on SNARE complex formation rate (Parlati et al., 1999). We found that the cytoplasmic domain of TI-VAMP, which comprises the NH_2-terminal domain plus the R-SNARE motif, had no effect on neurite outgrowth, whereas the NH_2-terminal domain alone strongly inhibited it. This demonstrates that the full cytoplasmic domain is inactive in vivo. The coiled-coiled domain of TI-VAMP bound more efficiently SNAP25 than the cytoplasmic domain by overlay assay. Therefore, our observations would favor a model in which the NH_2-terminal domain of TI-VAMP inhibits the capacity of the R-SNARE motif to form SNARE complexes and promote fusion, maybe because the NH_2-terminal domain folds over the R-SNARE motif or by a yet unknown mechanism. Cytosolic or membrane proteins can be expected to act on the NH_2-terminal domain of TI-VAMP to permit fusion at maximal rate. The inhibitory effect on neurite outgrowth resulting from expression of the NH_2-terminal domain of TI-VAMP could be due to the sequestration of such factor(s). Conversely, the activatory effect of the ΔNter-TIVAMP could be explained by the fact that it bypassed control by such factors. Hence, identifying the signal transduction pathway(s) and factors, able to activate TI-VAMP, will be of crucial importance to further understand how neurite outgrowth is controlled.

Finally, our finding that the NH_2-terminal domain of TI-VAMP plays an important function in the control of neurite outgrowth, suggests that this protein is a potential target of pharmacological agents that could modulate the activity of TI-VAMP by releasing the inhibition of this domain. Such agents could specifically activate TI-VAMP–mediated exocytosis thus stimulate neurite outgrowth. Once identified, such drugs could be used in the treatment of nerve traumatisms such as spinal cord injury.

References

Advani, R.J., B. Yang, R. Prekeris, K.C. Lee, J. Klumperman, and R.H. Scheller. 1999. VAMP-7 mediates vesicular transport from endosomes to lysosomes. *J. Cell Biol.* 146:765–775.

AhnertHilger, G., U. Kutay, I. Chahoud, T. Rapoport, and B. Wiedenmann. 1996. Synaptobrevin is essential for secretion but not for the development of synaptic processes. *Eur. J. Cell Biol.* 70:1–11.

Ayala, J., N. Touchot, A. Zahraoui, A. Tavitian, and A. Prochiantz. 1990. The product of rab2, a small GTP binding protein, increases neuronal adhesion, and neurite growth in vitro. *Neuron.* 4:797–805.

Bock, J.B., and R.H. Scheller. 1999. SNARE proteins mediate lipid bilayer fusion. *Proc. Natl. Acad. Sci. USA.* 96:12227–12229.

Boschert, U., C. O'Shaughnessy, R. Dickinson, M. Tessari, C. Bendotti, S. Catsicas, and E.M. Pich. 1996. Developmental and plasticity-related differential expression of two SNAP-25 isoforms in the rat brain. *J. Comp. Neurol.* 367:177–193.

Bradke, F., and C.G. Dotti. 1997. Neuronal polarity: vectorial cytoplasmic flow precedes axon formation. *Neuron.* 19:1175–1186.

Callebaut, I., G. Labesse, P. Durand, A. Poupon, L. Canard, J. Chomilier, B. Henrissat, and J.P. Mornon. 1997. Deciphering protein sequence information through hydrophobic cluster analysis (HCA): current status and perspectives. *Cell Mol. Life Sci.* 53:621–645.

Catsicas, S., G. Grenningloh, and E.M. Pich. 1994. Nerve-terminal proteins: to fuse to learn. *Trends Neurosci.* 17:368–373.

Chilcote, T.J., T. Galli, O. Mundigl, L. Edelmann, P.S. McPherson, K. Takei, and P. De Camilli. 1995. Cellubrevin and synaptobrevins: similar subcellular localization and biochemical properties in PC12 cells. *J. Cell Biol.* 129:219–231.

Coco, S., G. Raposo, S. Martinez, J.J. Fontaine, S. Takamori, A. Zahraoui, R. Jahn, M. Matteoli, D. Louvard, and T. Galli. 1999. Subcellular localization of tetanus neurotoxin-insensitive vesicle-associated membrane protein (VAMP)/VAMP7 in neuronal cells: Evidence for a novel membrane compartment. *J. Neurosci.* 19:9803–9812.

Cuff, J.A., M.E. Clamp, A.S. Siddiqui, M. Finlay, and G.J. Barton. 1998. JPred: a consensus secondary structure prediction server. *Bioinformatics.* 14:892–893.

D'Esposito, M., A. Ciccodicola, F. Gianfrancesco, T. Esposito, L. Flagiello, R. Mazzarella, D. Schlessinger, and M. D'Urso. 1996. A synaptobrevin-like gene in the Xq28 pseudoautosomal region undergoes X inactivation. *Nat. Genet.* 13:227–229.

Deitcher, D.L., A. Ueda, B.A. Stewart, R.W. Burgess, Y. Kidokoro, and T.L. Schwarz. 1998. Distinct requirements for evoked and spontaneous release of neurotransmitter are revealed by mutations in the *Drosophila* gene neuronal-synaptobrevin. *J. Neurosci.* 18:2028–2039.

Fernandez, I., J. Ubach, I. Dulubova, X.Y. Zhang, T.C. Sudhof, and J. Rizo. 1998. Three-dimensional structure of an evolutionarily conserved N-terminal domain of syntaxin 1A. *Cell.* 94:841–849.

Futerman, A.H., and G.A. Banker. 1996. The economics of neurite outgrowth—the addition of new membrane to growing axons. *Trends Neurosci.* 19:144–149.

Galli, T., E.P. Garcia, O. Mundigl, T.J. Chilcote, and P. DeCamilli. 1995. v- and t-SNAREs in neuronal exocytosis: a need for additional components to define sites of release. *Neuropharmacol.* 34:1351–1360.

Galli, T., A. Zahraoui, V.V. Vaidyanathan, G. Raposo, J.M. Tian, M. Karin, H. Niemann, and D. Louvard. 1998. A novel tetanus neurotoxin-insensitive vesicle-associated membrane protein in SNARE complexes of the apical plasma membrane of epithelial cells. *Mol. Biol. Cell.* 9:1437–1448.

Garcia, E.P., P.S. McPherson, T.J. Chilcote, K. Takei, and P. De Camilli. 1995. rbSec1A and B colocalize with syntaxin 1 and SNAP-25 throughout the axon, but are not in a stable complex with syntaxin. *J. Cell Biol.* 129:105–120.

Greene, L.A., and A.S. Tischler. 1976. Establishment of a noradrenergic clonal line of rat adrenal pheochromocytoma cells which respond to nerve growth factor. *Proc. Natl. Acad. Sci. USA.* 73:2424–2428.

Huber, L.A., P. Dupree, and C.G. Dotti. 1995. A deficiency of the small GTPase rab8 inhibits membrane traffic in developing neurons. *Mol. Cell Biol.* 15:918–924.

Ikonen, E., M. Tagaya, O. Ullrich, C. Montecucco, and K. Simons. 1995. Different requirements for NSF, SNAP, and rab proteins in apical and basolateral transport in MDCK cells. *Cell.* 81:571–580.

Jahn, R., and T.C. Sudhof. 1999. Membrane fusion and exocytosis. *Annu. Rev. Biochem.* 68:863–911.

Johannes, L., and T. Galli. 1998. Exocytosis: SNAREs drum up. *Eur. J. Neurosci.* 10:415–422.

Kobayashi, T., U.M. Vischer, C. Rosnoblet, C. Lebrand, M. Lindsay, R.G. Par-

ton, E.K.O. Kruithof, and J. Gruenberg. 2000. The tetraspanin CD63/lamp3 cycles between endocytic and secretory compartments in human endothelial cells. *Mol. Biol. Cell.* 11:1829–1843.

Lafont, F., P. Verkade, T. Galli, C. Wimmer, D. Louvard, and K. Simons. 1999. Raft association of SNAP receptors acting in apical trafficking in Madin-Darby canine kidney cells. *Proc. Natl. Acad. Sci. USA.* 96:3734–3738.

Leoni, C., A. Menegon, F. Benfenati, D. Toniolo, M. Pennuto, and F. Valtorta. 1999. Neurite extension occurs in the absence of regulated exocytosis in PC12 subclones. *Mol. Biol. Cell.* 10:2919–2931.

Li, S.H., A.L. Cheng, H. Li, and X.J. Li. 1999. Cellular defects and altered gene expression in PC12 cells stably expressing mutant huntingtin. *J. Neurosci.* 19: 5159–5172.

Luckenbill-Edds, L., C. Van Horn, and L.A. Greene. 1979. Fine structure of initial outgrowth of processes induced in a pheochromocytoma cell line (PC12) by nerve growth factor. *J. Neurocytol.* 8:493–511.

MaleticSavatic, M., R. Malinow, and K. Svoboda. 1999. Rapid dendritic morphogenesis in CA1 hippocampal dendrites induced by synaptic activity. *Science.* 283:1923–1927.

Nicholson, K.L., M. Munson, R.B. Miller, T.J. Filip, R. Fairman, and F.M. Hughson. 1998. Regulation of SNARE complex assembly by an N-terminal domain of the t-SNARE Sso1p. *Nat. Struct. Biol.* 5:793–802.

Nickel, W., T. Weber, J.A. McNew, F. Parlati, T.H. Sollner, and J.E. Rothman. 1999. Content mixing and membrane integrity during membrane fusion driven by pairing of isolated v-SNAREs and t-SNAREs. *Proc. Natl. Acad. Sci. USA.* 96:12571–12576.

Noel, J., G.S. Ralph, L. Pickard, J. Williams, E. Molnar, J.B. Uney, G.L. Collingridge, and J.M. Henley. 1999. Surface expression of AMPA receptors in hippocampal neurons is regulated by an NSF-dependent mechanism. *Neuron.* 23:365–376.

Nonet, M.L., O. Saifee, H.J. Zhao, J.B. Rand, and L.P. Wei. 1998. Synaptic transmission deficits in *Caenorhabditis elegans* synaptobrevin mutants. *J.*

Neurosci. 18:70–80.

Osen-Sand, A., M. Catsicas, J.K. Staple, K.A. Jones, G. Ayala, J. Knowles, G. Grenningloh, and S. Catsicas. 1993. Inhibition of axonal growth by SNAP-25 antisense oligonucleotides in vitro and in vivo. *Nature.* 364:445–448.

Osen-Sand, A., J.K. Staple, E. Naldi, G. Schiavo, O. Rossetto, S. Petitpierre, A. Malgaroli, C. Montecucco, and S. Catsicas. 1996. Common and distinct fusion proteins in axonal growth and transmitter release. *J. Comp. Neurol.* 367: 222–234.

Parlati, F., T. Weber, J.A. McNew, B. Westermann, T.H. Sollner, and J.E. Rothman. 1999. Rapid and efficient fusion of phospholipid vesicles by the alpha-helical core of a SNARE complex in the absence of an N-terminal regulatory domain. *Proc. Natl. Acad. Sci. USA.* 96:12565–12570.

Prochiantz, A. 1995. Neuronal polarity: giving neurons heads and tails. *Neuron.* 15:743–746.

Schagger, H., and G. von Jagow. 1987. Tricine-sodium dodecyl sulfate-polyacrylamide gel electrophoresis for the separation of proteins in the range from 1 to 100 kDa. *Anal. Biochem.* 166:368–379.

Shi, S.H., Y. Hayashi, R.S. Petralia, S.H. Zaman, R.J. Wenthold, K. Svoboda, and R. Malinow. 1999. Rapid spine delivery and redistribution of AMPA receptors after synaptic NMDA receptor activation. *Science.* 284:1811–1816.

Simons, K., and E. Ikonen. 1997. Functional rafts in cell membranes. *Nature.* 387:569–572.

Thiele, C., H.H. Gerdes, and W.B. Huttner. 1997. Protein secretion: puzzling receptors. *Curr. Biol.* 7:R496–R500.

Weber, T., B.V. Zemelman, J.A. McNew, B. Westermann, M. Gmachl, F. Parlati, T.H. Sollner, and J.E. Rothman. 1998. SNAREpins: minimal machinery for membrane fusion. *Cell.* 92:759–772.

Yao, R., M. Yoshihara, and H. Osada. 1997. Specific activation of a c-Jun NH_2-terminal kinase isoform and induction of neurite outgrowth in PC-12 cells by staurosporine. *J. Biol. Chem.* 272:18261–18266.